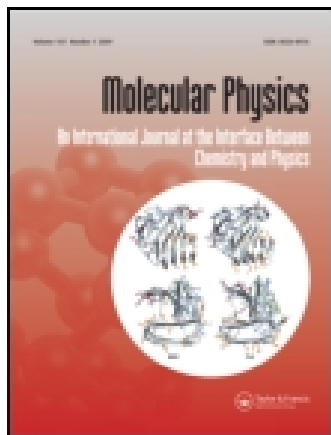


This article was downloaded by: [University of Otago]

On: 03 October 2014, At: 02:00

Publisher: Taylor & Francis

Informa Ltd Registered in England and Wales Registered Number: 1072954 Registered office: Mortimer House, 37-41 Mortimer Street, London W1T 3JH, UK



## Molecular Physics: An International Journal at the Interface Between Chemistry and Physics

Publication details, including instructions for authors and subscription information:

<http://www.tandfonline.com/loi/tmph20>

### A semiclassical dynamics study of the photoisomerization of methyl-substituted azobenzene

Shuai Yuan<sup>a</sup>, Weifeng Wu<sup>a</sup>, Zhaolin Wei<sup>a</sup>, Kunxian Shu<sup>a</sup>, Hong Tang<sup>a</sup>, Yusheng Dou<sup>a,b</sup> & Glenn V. Lo<sup>b</sup>

<sup>a</sup> Institute of Computational Chemistry, Chongqing University of Posts and Telecommunications, Chongqing 400065, China

<sup>b</sup> Department of Physical Sciences, Nicholls State University, PO Box 2022, Thibodaux, LA 70310, USA

Published online: 02 Nov 2010.

To cite this article: Shuai Yuan, Weifeng Wu, Zhaolin Wei, Kunxian Shu, Hong Tang, Yusheng Dou & Glenn V. Lo (2010) A semiclassical dynamics study of the photoisomerization of methyl-substituted azobenzene, *Molecular Physics: An International Journal at the Interface Between Chemistry and Physics*, 108:24, 3431-3441, DOI: [10.1080/00268976.2010.520755](https://doi.org/10.1080/00268976.2010.520755)

To link to this article: <http://dx.doi.org/10.1080/00268976.2010.520755>

PLEASE SCROLL DOWN FOR ARTICLE

Taylor & Francis makes every effort to ensure the accuracy of all the information (the "Content") contained in the publications on our platform. However, Taylor & Francis, our agents, and our licensors make no representations or warranties whatsoever as to the accuracy, completeness, or suitability for any purpose of the Content. Any opinions and views expressed in this publication are the opinions and views of the authors, and are not the views of or endorsed by Taylor & Francis. The accuracy of the Content should not be relied upon and should be independently verified with primary sources of information. Taylor and Francis shall not be liable for any losses, actions, claims, proceedings, demands, costs, expenses, damages, and other liabilities whatsoever or howsoever caused arising directly or indirectly in connection with, in relation to or arising out of the use of the Content.

This article may be used for research, teaching, and private study purposes. Any substantial or systematic reproduction, redistribution, reselling, loan, sub-licensing, systematic supply, or distribution in any form to anyone is expressly forbidden. Terms & Conditions of access and use can be found at <http://www.tandfonline.com/page/terms-and-conditions>

## RESEARCH ARTICLE

### A semiclassical dynamics study of the photoisomerization of methyl-substituted azobenzene

Shuai Yuan<sup>a</sup>, Weifeng Wu<sup>a</sup>, Zhaolin Wei<sup>a</sup>, Kunxian Shu<sup>a</sup>,  
Hong Tang<sup>a</sup>, Yusheng Dou<sup>ab\*</sup> and Glenn V. Lo<sup>b</sup>

<sup>a</sup>Institute of Computational Chemistry, Chongqing University of Posts and Telecommunications,  
Chongqing 400065, China; <sup>b</sup>Department of Physical Sciences, Nicholls State University,  
PO Box 2022, Thibodaux, LA 70310, USA

(Received 21 June 2010; final version received 27 August 2010)

A semiclassical dynamics simulation study is reported for a *trans*–*cis* photoisomerization cycle of four azo compounds, including azobenzene, 2-methylazobenzene, 2,6-dimethylazobenzene, and 2,2'-dimethylazobenzene. For both *trans* → *cis* and *cis* → *trans* isomerization processes, each compound is excited by a 50 fs (fwhm) laser pulse with a photon energy leading to a  $\pi\pi^*$  excitation. It is found that the compound in both cases follows a rotational path from reactant to product and that the isomerization dynamics is significantly affected by substitution. The relative times for completing a *trans*–*cis* isomerization cycle for four compounds, 2,6-dimethylazobenzene > 2,2-dimethylazobenzene and 2,6-dimethylazobenzene > 2-methylazobenzene > azobenzene, follow the same order as for the photoinduced formation of the surface relief grating of polymers based on these four compounds. The simulation results provide a basis for understanding the surface relief grating formation of azobenzene-based materials upon irradiation with laser beams.

**Keywords:** methyl substituted azobenzene; surface relief grating; inscription rate; photoisomerization

#### 1. Introduction

Azobenzene and its compounds have two isomers, *cis* and *trans*. The two isomers can convert reversibly when absorbing photons of appropriate energies [1]. It is this property that makes azobenzene and its derivatives potentially useful in many applications, including optical information storage, optical switching devices, and diffractive optical elements [2–4].

For practical applications, azobenzene or its derivatives are employed to form an azobenzene-based molecular film, called an azopolymer film. When exposed to two interference laser beams, a free azopolymer film was found to form a sinusoidal grating with regular periodicity [5–7]. This feature, called photoinduced surface relief grating (SRG) formation, is an important photomechanical effect and has attracted considerable research attention [8]. The formation of SRG results from mass transport in the surface, which is induced by many *trans*–*cis* isomerization cycles of azobenzene or its derivatives in the film [5–7,9–12]. It is therefore believed that a *trans*–*cis* photoisomerization cycle plays an important role in SRG formation.

Several investigations have been performed to examine the effects of the structural features of azobenzene or its compounds on the SRG formation process. The structural features studied include the size of the azobenzene group [13,14], the amount of azobenzene or its derivatives embedded in a film [15–18], the length of the side chain [19–22], and the different substituents in the azobenzene group [23–26]. These studies reveal that the SRG formation process is sensitive to chemical alteration of the azobenzene group. General trends regarding how the chemical alterations affect the SRG formation process provide a guideline for material researchers to construct an appropriate azobenzene-based polymer for a specific purpose.

In experimental investigations, an azobenzene-based polymer film is irradiated by a continuous-wave (cw) laser beam. The SRG formation therefore involves repeated *trans*–*cis* isomerization cycles. A better description of this macroscopic phenomenon requires a full understanding of the mechanism of a fundamental *trans*–*cis* isomerization cycle. Despite significant research progress in the field, the

\*Corresponding author. Email: yusheng.dou@nicholls.edu

question of how the chemical modifications of the azobenzene group shape the mechanism of the *trans-cis* photoisomerization of azobenzene remains unanswered.

The isomerization of azobenzene from each isomer can occur following an excitation to either the first ( $n \rightarrow \pi^*$ ,  $S_1$ ) or the second ( $\pi \rightarrow \pi^*$ ,  $S_2$ ) excited state. However, the photoisomerization quantum yield for  $S_1$  is significantly greater than that for  $S_2$  for each isomer [27]. Absorption spectroscopy measurements for excitation to the first excited state have shown that the formation of the dominant photoproduct occurs with 170 fs for *cis*-azobenzene [28] and 600 fs for *trans*-azobenzene [29]. It has been suggested that isomerization proceeds along different pathways for different excitations. The azobenzene molecule takes an inversion path from the reactant to the product for the  $n \rightarrow \pi^*$  excitation and a rotation path for the  $\pi \rightarrow \pi^*$  excitation [30,31]. A third reaction path involving the simultaneous bending of both C–N–N bond angles, called the concerted inversion pathway, has been proposed recently [32]. We have previously performed a semiclassical dynamics simulation study of the isomerization of *trans*-azobenzene initiated by an ultrashort laser pulse [33]. The simulation results provide many details about the mechanism of this reaction.

In this report, we describe a semiclassical dynamics investigation of a *trans-cis* isomerization cycle of azobenzene and three derivatives following excitation by an ultrafast laser pulse. The results of this study provide a microscopic picture for the photoinduced formation of the surface relief grating of an azobenzene-based polymer film.

## 2. Methodology

We performed the dynamics simulations using the semiclassical electron–radiation–ion dynamics (SERID) method. In this approach, valence electrons are calculated by the time-dependent Schrödinger equation while both the radiation field and the motion of the nuclei are treated by the classical approximation. A detailed description of this technique has been published elsewhere [34,35] and here a brief explanation is presented. The one-electron states are updated by solving the time-dependent Schrödinger equation at each time step (typically 0.05 fs in duration) in a non-orthogonal basis,

$$i\hbar \frac{\partial \Psi_j}{\partial t} = \mathbf{S}^{-1} \cdot \mathbf{H} \cdot \Psi_j, \quad (1)$$

where  $\mathbf{S}$  is the overlap matrix for atomic orbitals. The laser pulse, characterized by the vector potential

$\mathbf{A}$ , is coupled to the Hamiltonian via the time-dependent Peierls substitution [36,37]

$$H_{ab}(\mathbf{X} - \mathbf{X}') = H_{ab}^0(\mathbf{X} - \mathbf{X}') \exp\left(\frac{iq}{\hbar c} \mathbf{A} \cdot (\mathbf{X} - \mathbf{X}')\right), \quad (2)$$

where  $H_{ab}(\mathbf{X} - \mathbf{X}')$  is the Hamiltonian matrix element for basis functions  $a$  and  $b$  on atoms at  $\mathbf{X}$  and  $\mathbf{X}'$  respectively, and  $q = -e$  is the charge of the electron.

The Hamiltonian matrix elements, overlap matrix elements, and repulsive energy are calculated with the density-functional-based tight bonding (DFTB) method [38,39]. The DFTB method essentially has the same strengths and limitations as TD-DFT. For example, the bonding is well-described but the excited-state energies are typically too low. In this study, we matched the central photon energy of the laser pulse to the relevant density-functional (rather than experimental) excitation energy. This should not have a significant effect on the interpretation of the results.

The forces acting on ions are computed by the Ehrenfest equation:

$$M_l \frac{d^2 X_{l\alpha}}{dt^2} = -\frac{1}{2} \sum_j \Psi_j^+ \cdot \left( \frac{\partial \mathbf{H}}{\partial X_{l\alpha}} - i\hbar \frac{1}{2} \frac{\partial \mathbf{S}}{\partial X_{l\alpha}} \cdot \frac{\partial}{\partial t} \right) \cdot \Psi_j - \partial U_{\text{rep}} / \partial X_{l\alpha}, \quad (3)$$

where  $U_{\text{rep}}$  is the effective nuclear–nuclear repulsive potential and  $X_{l\alpha} = \langle \hat{X}_{l\alpha} \rangle$  is the expectation value of the time-dependent Heisenberg operator for the  $\alpha$  coordinate of the nucleus labelled  $l$  (with  $\alpha = x, y, z$ ). Equation (3) is obtained by neglecting the terms of second and higher order in the quantum fluctuations  $\hat{X} - \langle \hat{X}_{l\alpha} \rangle$  in the exact Ehrenfest theorem.

A unitary algorithm obtained from the equation for the time evolution operator [40] is used to solve the time-dependent Schrödinger Equation (1). Equation (3) is numerically integrated with the velocity Verlet algorithm. A time step of 50 attoseconds was used for this study and energy conservation was then found to hold better than 1 part in  $10^6$  in a 1 ps simulation for the methyl-group-substituted azobenzene molecule at 298 K.

The present model does not assume the validity of the Born–Oppenheimer (or adiabatic) approximation, in which the various terms in the Born–Oppenheimer expansion [41–45],

$$\Psi^{\text{total}}(X_n, x_e, t) = \sum_i \Psi_i^n(X_n, t) \Psi_i^e(x_e, X_n), \quad (4)$$

are postulated to evolve independently of one another. In fact, the present approach includes and clearly exhibits non-adiabatic effects, which become extremely

strong and of dominant importance when two or more Born–Oppenheimer terms, or ‘potential energy surfaces’, approach each other in energy. In the present method, this failure of the Born–Oppenheimer approximation emerges automatically during the course of a simulation, as can be seen in results such as those of Figure 8 and in many other results in our earlier paper [34,35].

In this work we examine the dynamics of the *trans*–*cis* photoisomerization of azobenzene and three methyl-substituted compounds of azobenzene, including 2-methylazobenzene, 2,6-dimethylazobenzene, and 2,2'-dimethylazobenzene. The ground-state geometry of each was determined in a 1000 fs simulation at 298 K. The geometry parameters, including bond lengths, bond angles, and dihedral angles as well as energies, were found to be consistent with either published values [46–49] or those obtained by optimal structure calculation at the B3LYP/6-31G\* level. For the generation of initial geometries for the dynamics simulation, each geometry was simulated for an additional 2000 fs without the application of any laser pulse. From each trajectory, 20 geometries taken at equal time intervals were used as starting geometries for any laser pulse intensity selection.

The characteristics of the laser pulses used for the excitation of each molecule are given in Table SM1 (Supplementary Online Material). All pulses have a Gaussian profile. The energy selected for each molecule makes a best non-resonant excitation of electrons from the HOMO–1 to the LUMO, which corresponds to a  $\pi\pi^*$  excitation. The fluence was selected so that the force acting on the nuclei was large enough to produce isomerization, but not break any chemical bonds; the values determined were of the same order as those used in the isomerization experiments [50,51]. The simulation at each laser pulse was run for several tens of trajectories. Each trajectory led to the formation of either product or reactant [52]. All trajectories leading to the formation of product for each methyl-substituted azobenzene show similar features and our presentations and discussions are based on a typical trajectory for each compound, but the differences between this trajectory and others are briefly described in a later paragraph.

### 3. Results and discussions

#### 3.1. *Trans* → *cis* isomerization

The time dependence of the C–N–N–C dihedral angle and a few snapshots taken at different times from the simulation of 2,2-dimethylazobenzene are presented in Figure 1. Starting with the *trans* structure (the 180°

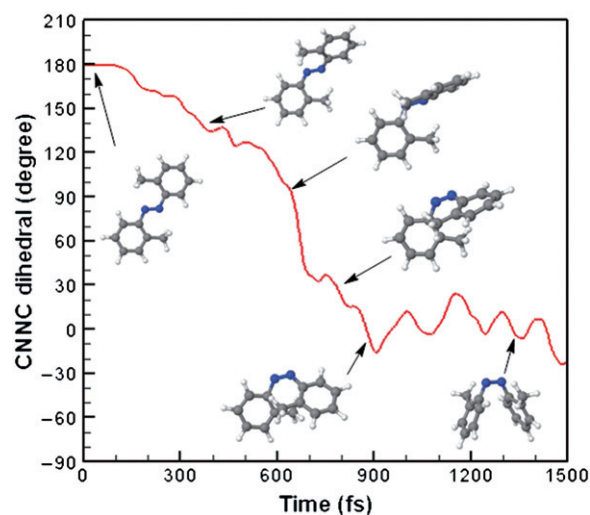


Figure 1. Variations with time of the C–N–N–C dihedral angle of *trans* 2, 2'-dimethylazobenzene. Few snapshots taken at different times from the simulation are also included.

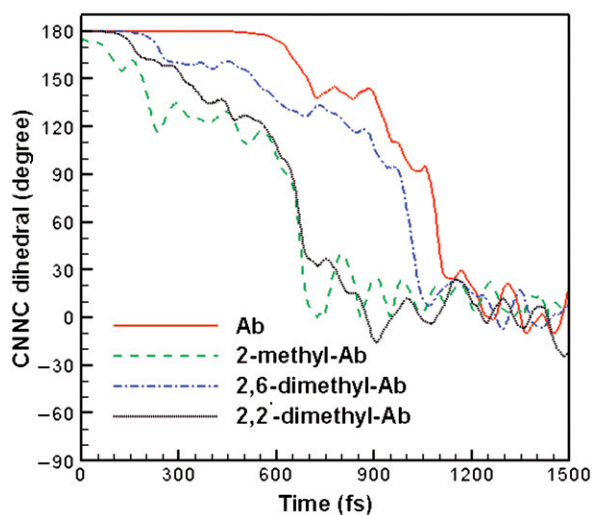


Figure 2. Variations with time of the C–N–N–C dihedral angles of *trans* azobenzene, *trans* 2-methylazobenzene, *trans* 2,6-dimethylazobenzene, and *trans* 2,2'-dimethylazobenzene subjected to laser irradiation with a 50 fs (fwhm) duration. This laser pulse induces a  $\pi\pi^*$  excitation.

dihedral angle), 2,2-dimethylazobenzene is found to start rotating about the N–N bond about 100 fs after laser pulse irradiation. It reaches the twisted structure (90° dihedral angle) at about 600 fs. Shortly before 900 fs, the *cis* structure (0° dihedral angle) is obtained; the molecule then fluctuates about this geometry through the end of the simulation. The smooth variation of the dihedral angle suggests that the isomerization follows a rotation path from *trans* to *cis*.

Figure 2 demonstrates the time dependence of the dihedral angle for the four azo compounds. Clearly,

Table 1. Times of some critical events observed in the trajectory leading to the isomerization from *trans* to *cis*.

Molecule	$t_1$ (fs) <sup>a</sup>	$t_2$ (fs) <sup>b</sup>	$t_3$ (fs) <sup>c</sup>	$t_2 - t_1$	$t_3 - t_1$	$t_3 - t_2$
Azobenzene	546	1062	1228	516	682	166
2-Methylazobenzene	20	618	730	598	710	112
2,6-Dimethylazobenzene	146	922	1070	776	924	148
2,2'-Dimethylazobenzene	96	612	726	516	630	114

Notes: <sup>a</sup> $t_1$  is defined as the time of the beginning of isomerization.

<sup>b</sup> $t_2$  is defined as the time of the transfer of electrons to the electronic ground state; it also can be regarded as the lifetime of the excited state.

<sup>c</sup> $t_3$  is defined as the time of the formation of *cis* isomers.

*trans* to *cis* isomerization follows the laser excitation of each compound. However, the conversion times are different. For example, azobenzene starts to rotate about the N–N bond after 546 fs and the *cis* isomer is obtained after 1228 fs. In other words, it takes 682 fs for azobenzene to rotate from *trans* to *cis*. On the other hand, 2,6-dimethylazobenzene begins its rotation about the N–N bond at around 146 fs after the laser pulse and forms the *cis* structure at about 1070 fs. This process takes about 924 fs. Table 1 summarizes these critical times in the photoisomerization processes for azobenzene and all compounds. The isomerization time here is defined as the time difference between the formation of the *cis* isomer and the beginning of isomerization rather than the beginning of laser irradiation. The times for completing *trans* → *cis* isomerization ( $t_3 - t_1$  in Table 1) are in the order: 2,6-dimethylazobenzene > 2,2-dimethylazobenzene and 2,6-dimethylazobenzene > 2-methylazobenzene > azobenzene. Therefore, rates of rotation (degrees per femtosecond) about the N–N bond are in the order: 2,6-dimethylazobenzene < 2,2-dimethylazobenzene and 2,6-dimethylazobenzene < 2-methylazobenzene < azobenzene.

To study the relation between the methyl substitution and the inscription rates of SRG, Wang's team [25] synthesized a series of polymers functionalized with methyl-substituted azobenzene chromophores, including BP-AZ-NT, BP-3-AZ-NT, BP-35-AZ-NT, and BP-3-AZ-mNT, as listed in Figure 3. Their results show that the inscription rates decrease as the number of methyl substituents increases and that two methyl groups substituted at two phenyls have a more significant effect than when substituted at just one phenyl. They found that the inscription rates of methyl-substituted azopolymers have the following trends: BP-AZ-NT > BP-3-AZ-NT > BP-3-AZ-NT and BP-3-AZ-mNT > BP-35-AZ-NT. The functional group substitutions in four methyl-substituted azopolymer molecules is analogous to the substitutions in azobenzene, 2-methylazobenzene, 2,6-dimethylazobenzene, and 2,2'-dimethylazobenzene, respectively.

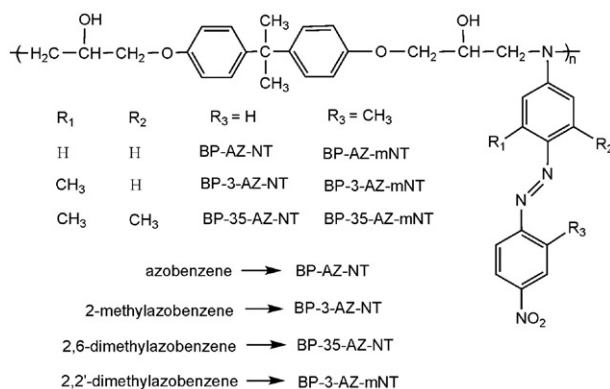


Figure 3. Molecular structures and abbreviations of methyl-substituted azopolymers.

As shown in Table 1, the rotation rates of the four compounds around the N–N bond have the same trends as the inscription rates of the four represented azopolymers.

The isomerization time is defined as the time period from the beginning of the rotation, rather than from the beginning of laser irradiation, to the completion of the isomerization. This definition enables us to directly compare the simulation results with the experimental observations since the SRG formation process is closely related to the molecular motions.

Showing the variations with time of the  $C_1$ –N–N and  $C'_1$ –N–N bond angles, together with the variation of the dihedral angle, provides more detailed information about the rotational dynamics. Comparing these angles at different times, we find several impressive features. (1) The maximum bond angle observed in the isomerization processes for all four compounds is as large as  $156^\circ$ , as shown in Figure 4(b). However, none of the bond angles is anywhere near  $180^\circ$ , indicating that each reaction takes a rotational path. (2) The changes in the dihedral angles are almost exclusively related to the expansion in either or both C–N–N bond angles. This suggests that the expansion in C–N–N

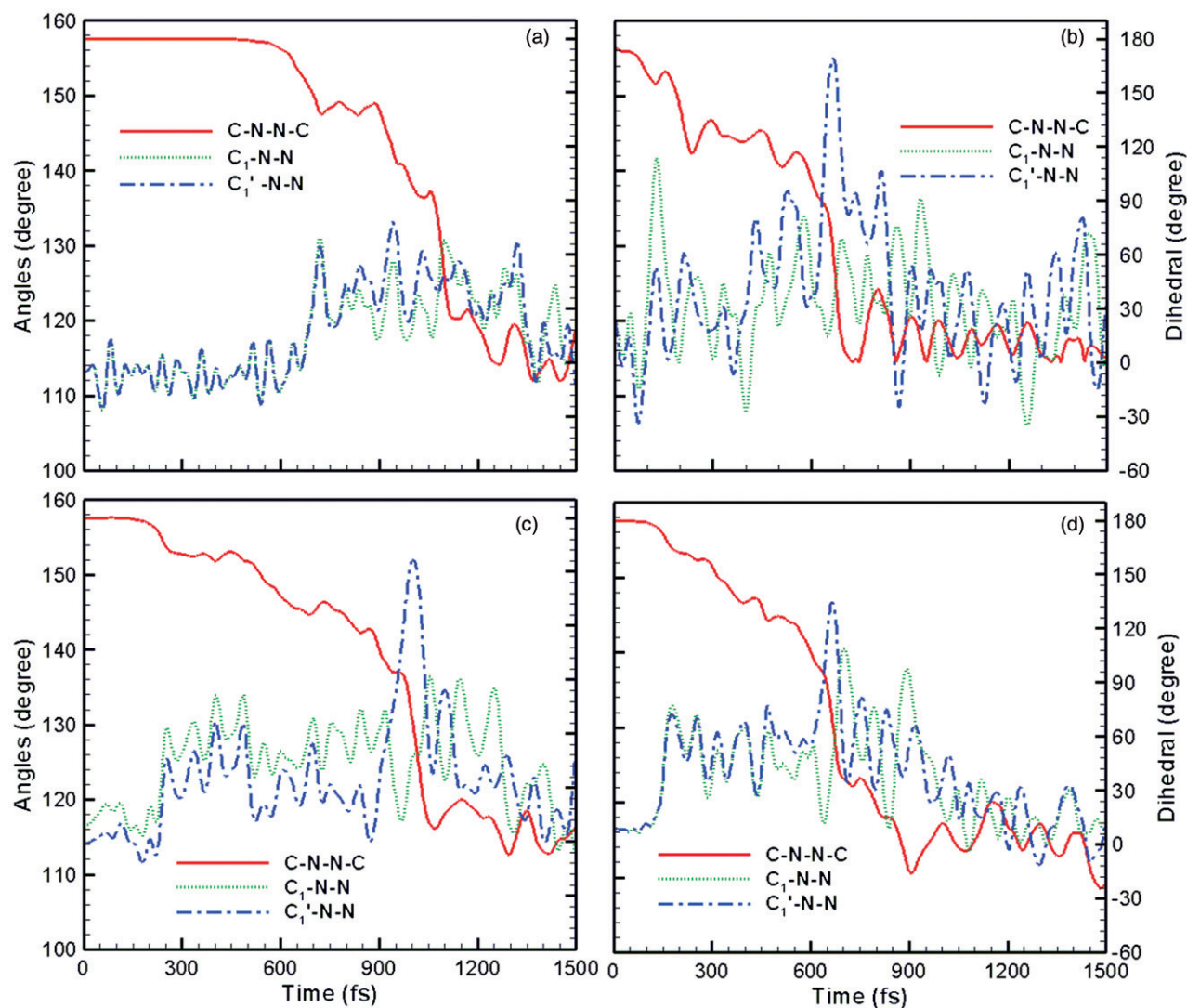


Figure 4. Variations with time of the  $C_1$ -N-N,  $C_1'$ -N-N angles and the C-N-N-C dihedral angle for (a) *trans* azobenzene, (b) *trans* 2-methylazobenzene, (c) *trans* 2,6-dimethylazobenzene, and (d) *trans* 2,2'-dimethylazobenzene.

angles facilitates the rotation of the compound about the N–N bond because it leads to more available space between the two phenyl rings. (3) After methyl-substituted azobenzenes form the *cis* structure, the bond angles return to their initial values and fluctuate about these values until the end of the simulations. This last feature demonstrates that each compound completes a *trans* to *cis* isomerization process. Molecular structures at  $t = 0$  fs and at  $t = t_1$  (time for a molecule to rotate about the N–N bond) are given in Figures 5 and 6 for each compound. It is seen that the two C–N–N angles for each molecule are greater at  $t_1$  than at  $t_0$ , indicating that before rotating about the N–N bond, each molecule takes some time to widen its  $C_1$ –N–N and/or  $C_1'$ –N–N bond angles to enable the

rotation to proceed. The larger the bond angle at  $t_0$ , the sooner the rotation starts. For the four compounds, the initial values of the two bond angles are in the following order: azobenzene < 2,6-dimethylazobenzene < 2,2'-dimethylazobenzene < 2-methylazobenzene. This is the same as the order for the beginning times ( $t_1$ ) of the rotation about the N–N bond, as shown in Table 1.

The electronic populations of the frontier molecular orbitals are plotted in Figure 7 for 2,2'-dimethylazobenzene from 0 fs to 100 fs and in Figure 8 for the four compounds over a longer time scale. At about 65 fs after the application of the laser pulse, approximately one electron is promoted from the HOMO–1 to the LUMO. This  $\pi\pi^*$  excitation brings the molecule

to an electronically excited state. Immediately after 70 fs, one finds relaxation of electrons from the HOMO to the HOMO-1. This leads to a switch from  $\pi\pi^*$  to  $n\pi^*$  excitation, a transfer of the excited

molecule from one excited state to another excited state. At the end of the laser pulse, roughly one electron remains at the LUMO and one hole stays at the HOMO. The four molecules show similar

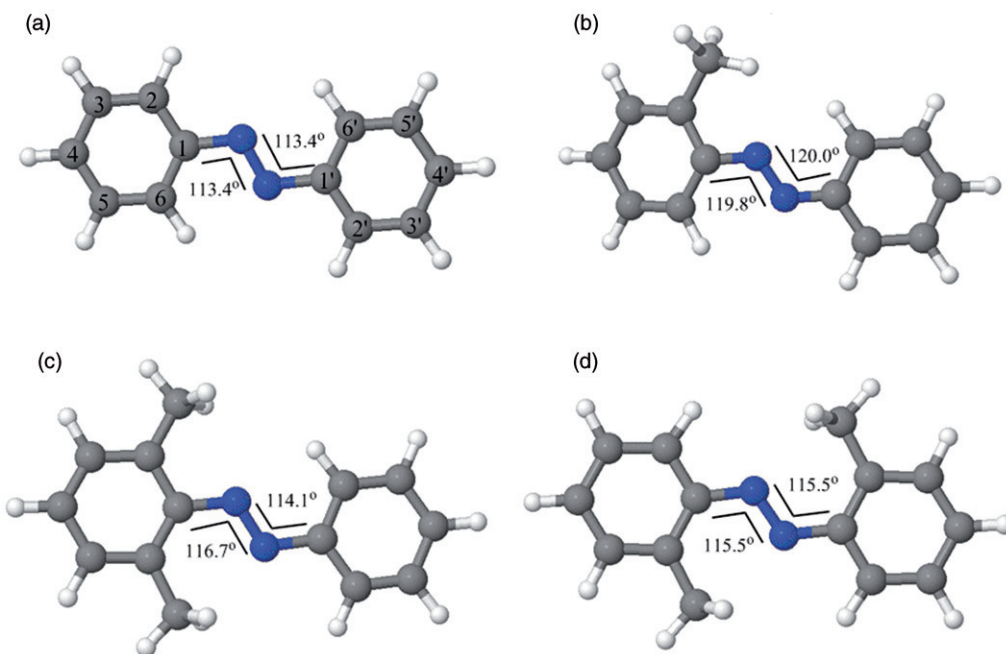


Figure 5. Molecular structures of (a) *trans* azobenzene, (b) *trans* 2-methylazobenzene, (c) *trans* 2,6-dimethylazobenzene, and (d) *trans* 2,2'-dimethylazobenzene at  $t = 0$  fs.

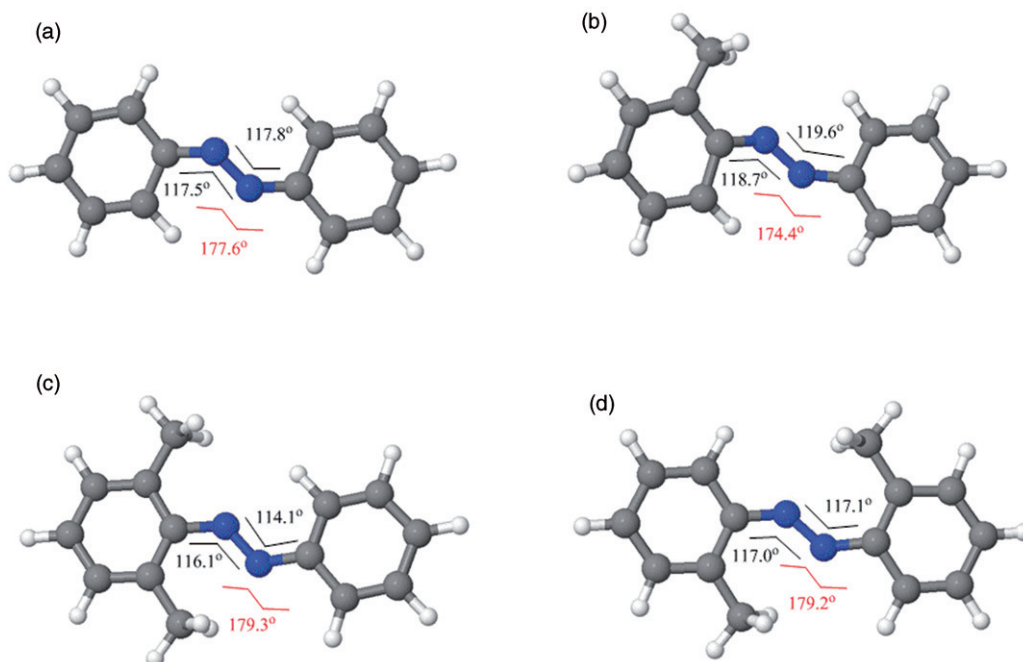


Figure 6. Molecular structures of (a) azobenzene, (b) 2-methylazobenzene, (c) 2,6-dimethylazobenzene, and (d) 2,2'-dimethylazobenzene at the beginning of rotation about the N-N bond.

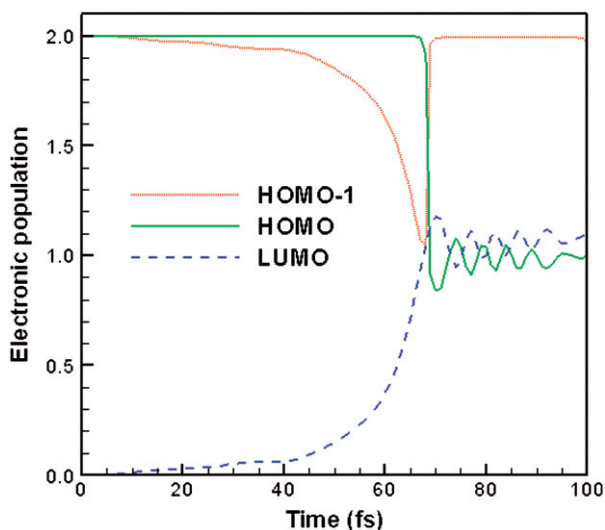


Figure 7. Variations with time of the electronic populations of the HOMO-1, HOMO, and LUMO of *trans* 2, 2'-dimethylazobenzene from 0 fs to 100 fs.

variation in the electronic population of the frontier molecular orbitals. Figure 8 reveals that there is a substantial de-excitation of electrons from the LUMO to the HOMO for each compound after laser excitation. The de-excitation times are listed in Table 1. This de-excitation eventually brings the excited molecule to the electronic ground state.

The energies of the HOMO-1, HOMO and LUMO are plotted in Figure 9 for 2,2'-dimethylazobenzene from 0 fs to 100 fs. Similar plots for the four compounds are presented in Figure 10 over a longer time scale. The 2,2'-dimethylazobenzene molecule has a cross between the HOMO and HOMO-1 level shortly before 70 fs. This crossing leads to changes in the electronic populations of the HOMO and HOMO-1, as shown in Figure 7. A similar crossing is also observed for each of the other three compounds. Another impressive feature in the energy variations of the frontier molecular orbitals, as seen in Figure 10,

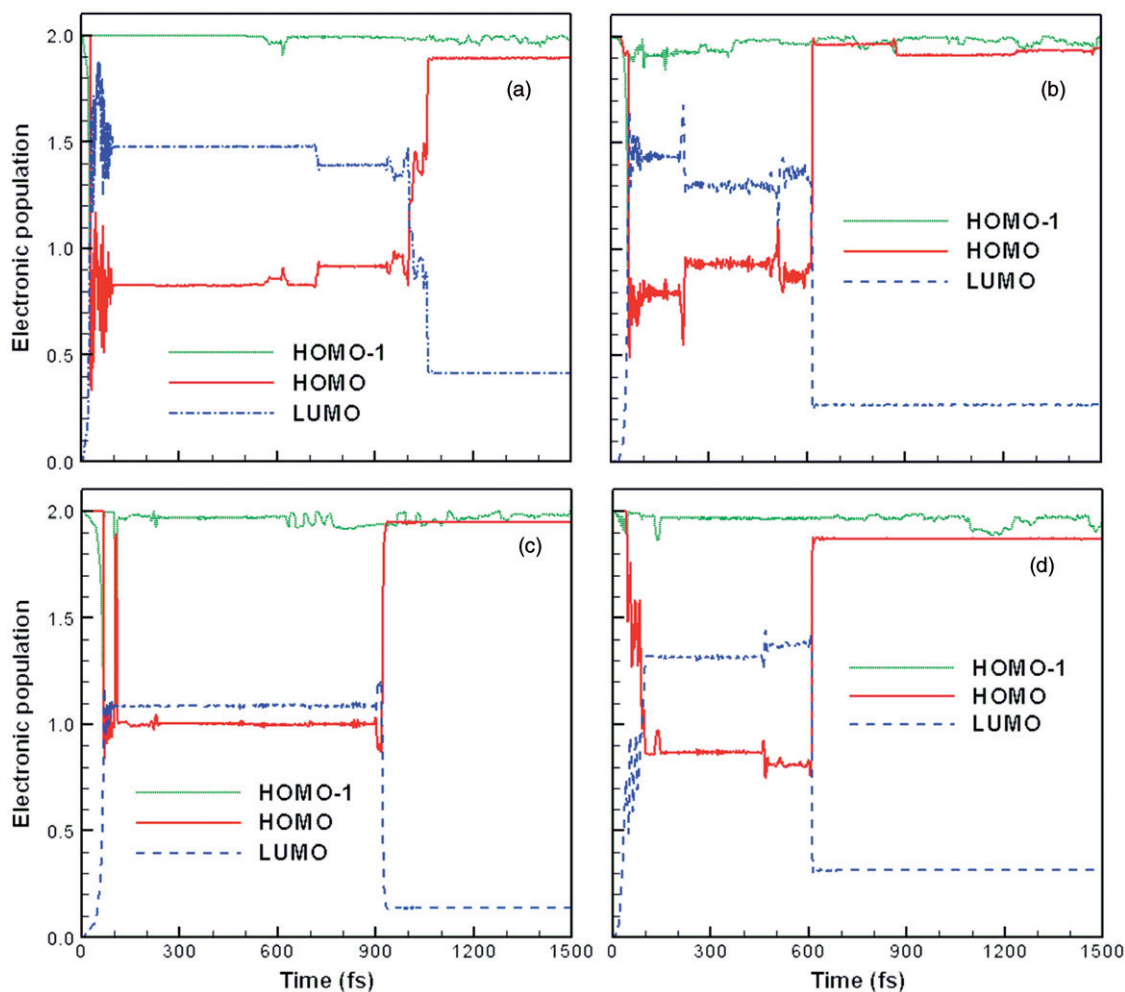


Figure 8. Variations with time of the electronic populations of the HOMO-1, HOMO, LUMO of (a) *trans* azobenzene, (b) *trans* 2-methylazobenzene, (c) *trans* 2,6-dimethylazobenzene and (d) *trans* 2,2'-dimethylazobenzene from 0 fs to 1500 fs.

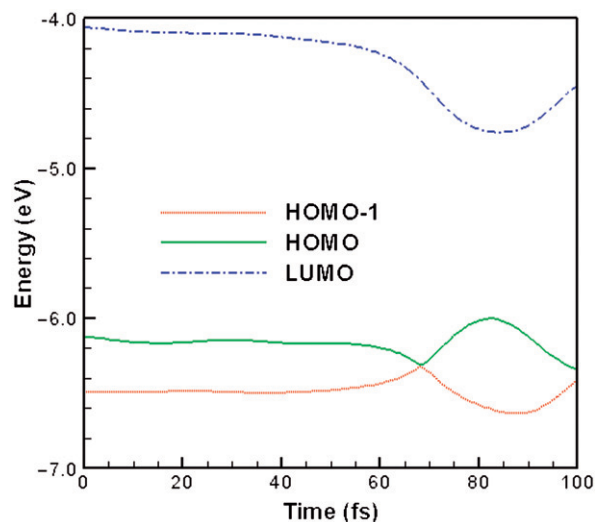


Figure 9. Energy variations with time of the HOMO-1, HOMO, and LUMO of *trans* 2, 2'-dimethylazobenzene.

is a rapid rise in the HOMO level at 546 fs for azobenzene, 20 fs for 2-methylazobenzene, 146 fs for 2,6-dimethylazobenzene, and 96 fs for 2,2'-dimethylazobenzene. This rapid rise in the HOMO energy occurs at the time when the rotation about the N–N bond starts. This observation suggests that the HOMO level is tremendously altered by the molecular rotation and bond angle bending. Thereafter, one finds one or more avoided crossings between the HOMO and LUMO levels for each compound. These avoided crossings lead to the transfers of electrons from the LUMO to the HOMO, which bring the excited compounds to the electronic ground state. The times when these avoided crossings occur are listed as  $t_2$  in Table 1. If more than one avoided crossing is observed, the time for the last is recorded.

Figure 11 presents the molecular structures of the four compounds at the last avoided crossing. These

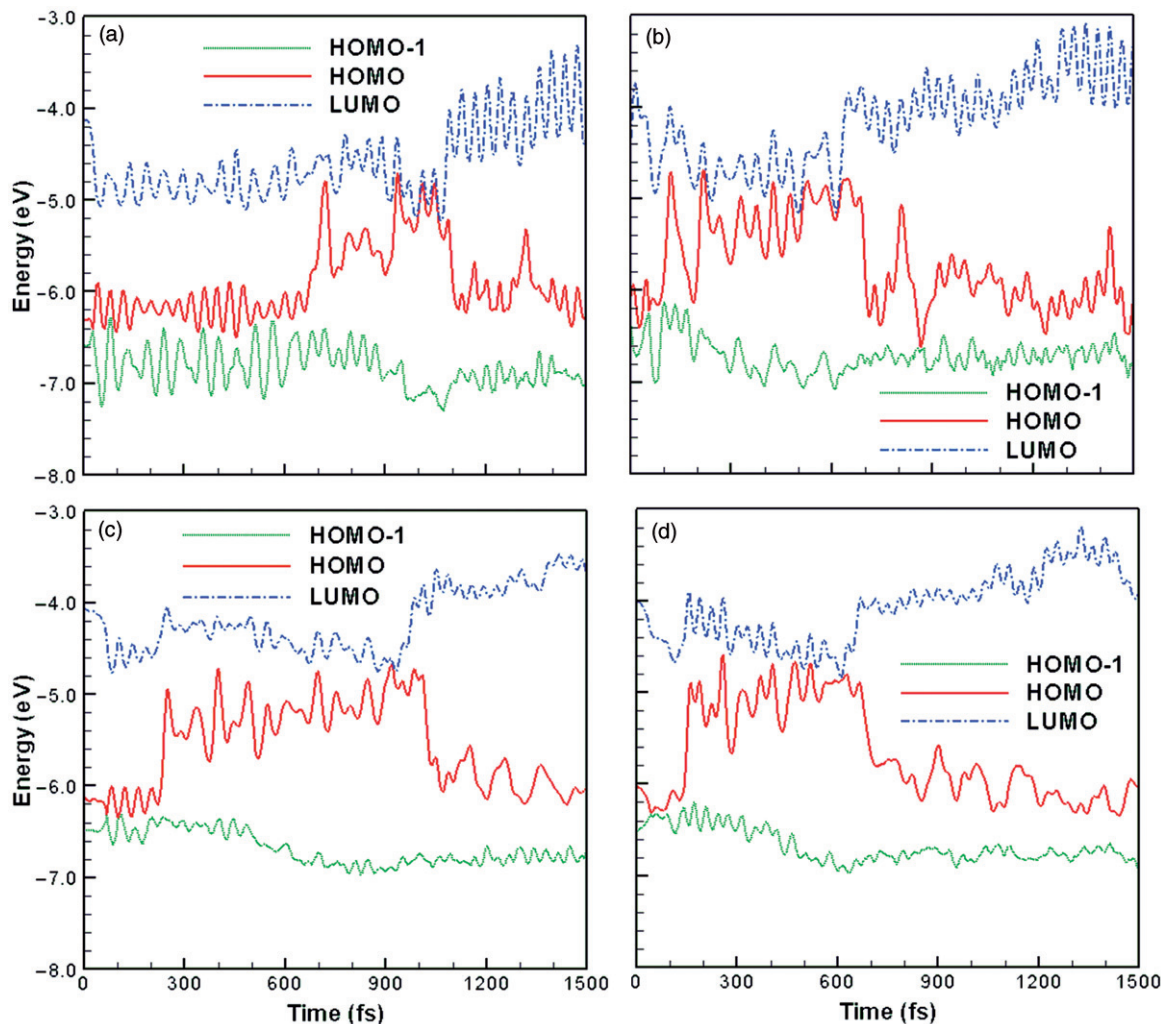


Figure 10. Variation with time of the energies of the HOMO-1, HOMO, and LUMO of (a) *trans* azobenzene, (b) *trans* 2-methylazobenzene, (c) *trans* 2,6-dimethylazobenzene, and (d) *trans* 2,2'-dimethylazobenzene.

structures are significantly different from each other, although each molecule has a roughly twisted structure. For example, the dihedral angle is  $94.02^\circ$  for azobenzene,  $94.62^\circ$  for 2-methylazobenzene,  $99.19^\circ$  for 2,6-dimethylazobenzene, and  $102.59^\circ$  for 2,2'-dimethylazobenzene. The bond angles C–N–N and N–N–C are also considerably different. The differences in the times of the last avoided crossings and the molecular structures at the avoided crossings are closely related to the different methyl substitution of azobenzene. The time differences between  $t_2$  and  $t_1$  are of the same order as those between  $t_3$  and  $t_1$ , as seen in Table 1. After dropping to the electronic ground state, methyl-substituted azobenzene moves quickly along a barrierless reaction path and becomes the *cis* isomer in about 100–200 fs. The time for this process is equal to  $t_3 - t_2$ , which is listed in Table 1 for each compound. There is no obvious relation between the  $t_3 - t_2$  times and different substitutions. However, the small values of  $t_3 - t_2$  do not alter the order of the reaction times from the reactants to the products for the four molecules discussed above.

Other trajectories of each compound show slightly different time scales for each process. However, the time order for the *trans* to *cis* isomerization remains the same and therefore the above discussions are valid.

### 3.2. *cis* $\rightarrow$ *trans* Isomerization

The variations of the dihedral angles with time are presented in Figure 12 for the *cis* to *trans* isomerization of the four compounds. Each compound begins to rotate about the N–N bond as soon as the laser pulse is applied. However, the four compounds take slightly different times to complete the isomerization. The *cis* isomer becomes the *trans* isomer at 550 fs, 564 fs, 848 fs, and 593 fs, respectively, for azobenzene, 2-methylazobenzene, 2,6-dimethylazobenzene and 2,2'-dimethylazobenzene. This gives the following order of the rotation rates (degrees per femtosecond) about the N–N bond: 2,6-dimethylazobenzene < 2,2'-dimethylazobenzene and 2,6-dimethylazobenzene < 2-methylazobenzene < azobenzene. This is the same order obtained for the *trans* to *cis* isomerization.

By combining the time scales from the *trans* to *cis* and those from *cis* to *trans*, one finds the following order for the rotation rates about the N–N bond for the four azo compounds: 2,6-dimethylazobenzene < 2,2'-dimethylazobenzene and 2,6-dimethylazobenzene < 2-methylazobenzene < azobenzene. This is the same as the experimentally observed order for the surface relief grating rates of the four represented methyl-substituted azopolymers. It is therefore concluded that the surface relief grating rate of an azobenzene-based molecular film is predominately

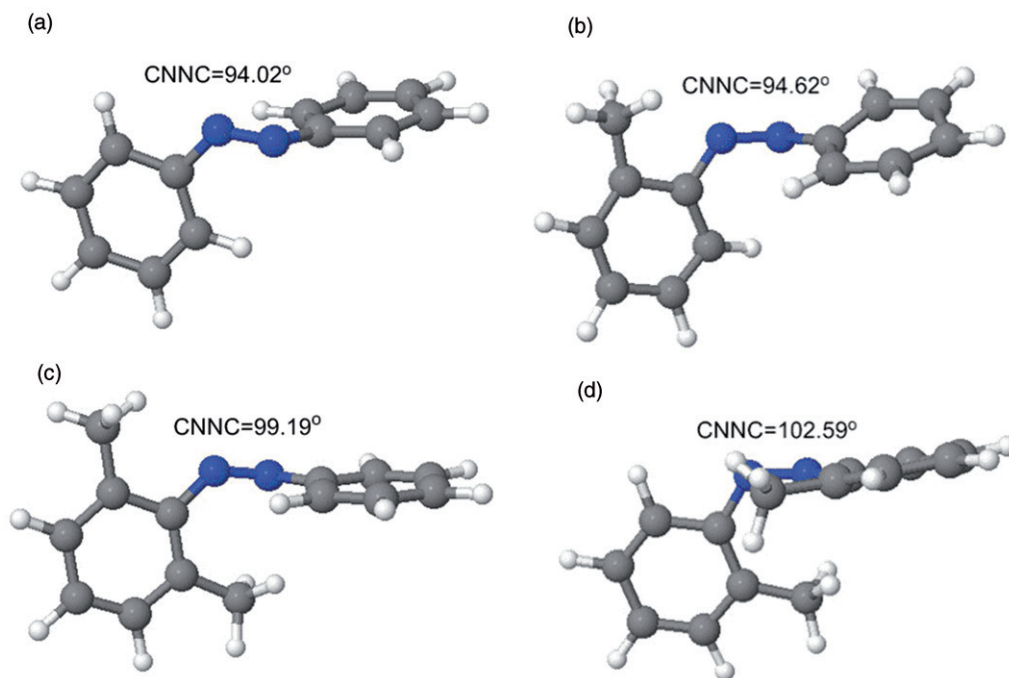


Figure 11. The molecular structures at the avoided crossing for (a) *trans* azobenzene, (b) *trans* 2-methylazobenzene, (c) *trans* 2,6-dimethylazobenzene, and (d) *trans* 2,2'-dimethylazobenzene.

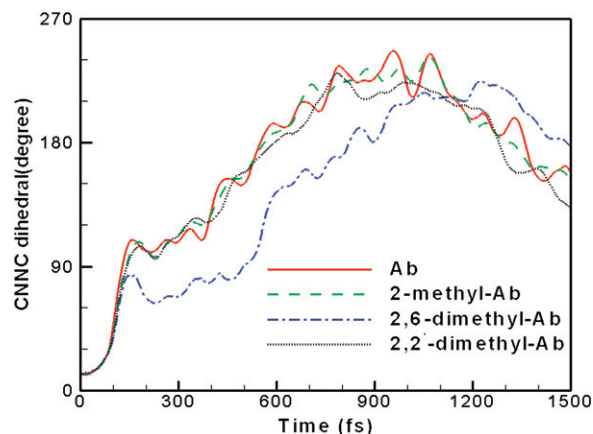


Figure 12. Variations with time of the C-N-N-C torsional angles of *cis* azobenzene, *cis* 2-methylazobenzene, *cis* 2,6-dimethylazobenzene, and *cis* 2,2'-dimethylazobenzene subjected to laser irradiation with a 50 fs (fwhm) duration. This laser pulse induces a  $\pi\pi^*$  excitation.

determined by the time scale of the isomerization process of the azopolymer.

#### 4. Summary and remarks

We have presented a detailed dynamics simulation study of a *cis-trans* isomerization cycle of azobenzene and three derivatives of azobenzene, including azobenzene, 2-methylazobenzene, 2,6-dimethylazobenzene, and 2,2'-dimethylazobenzene, and compared the photoisomerization times obtained by the simulation and the inscription rates of the surface relief grating of the four represented methyl-substituted azopolymers, called BP-AZ-NT, BP-3-AZ-NT, BP-35-AZ-NT, and BP-3-AZ-mNT. We find that the rotation rates (degrees per femtosecond) about the N-N bond from *trans* to *cis* and then back to *trans* for the four compounds are in the order: 2,6-dimethylazobenzene < 2,2'-dimethylazobenzene and 2,6-dimethylazobenzene < 2-methylazobenzene < azobenzene. This order is consistent with the experimentally observed order for the surface relief grating rates of the corresponding methyl-substituted azopolymers.

It should be noted that azobenzene-based polymers, such as BP-AZ-NT, BP-3-AZ-NT, BP-35-AZ-NT, and BP-3-AZ-mNT, are much larger in size than their corresponding molecules studied in the simulations (azobenzene, 2-methylazobenzene, 2,6-dimethylazobenzene, and 2,2'-dimethylazobenzene). The time scales for a *trans-cis* photoisomerization cycle of the bigger molecules must be significantly different from those for the simple methyl-substituted azobenzenes. However, the trends regarding how the methyl

substitutions affect the mechanism of a photoisomerization process remain valid.

#### Acknowledgements

We acknowledge support by the National Natural Science Foundation of China (grant 20773168), the Project of the Science Technology Foundation of Chongqing Education Committee (No. KJ100507) and the Research Fund of Chongqing University of Posts and Telecommunications (A2006-81 and A2009-63). Acknowledgment is also made to the donors of The American Chemical Society Petroleum Research Fund for support of this research at Nicholls State University.

#### Note

Supplementary material can be viewed online.

#### References

- [1] Z. Sekkat and W. Knoll, editors, *Photoreactive Organic Thin Film* (Academic Press, San Diego, 2002), Chapt. 1 and 14.
- [2] T. Ikeda and O. Tsutsumi, *Science* **268**, 1873 (1995).
- [3] A.N. Shipway and I. Willner, *Acc. Chem. Res.* **34**, 421 (2001).
- [4] Z.F. Liu, K. Hashimoto and A. Fujishima, *Nature* **347**, 658 (1990).
- [5] G.S. Kumar and D.C. Neckers, *Chem. Rev.* **89**, 1915 (1989).
- [6] P. Rochon, E. Batalla and A. Natansohn, *Appl. Phys. Lett.* **66**, 136 (1995).
- [7] D.Y. Kim, S.K. Tripathy, L. Li and J. Kumar, *Appl. Phys. Lett.* **66**, 1166 (1995).
- [8] A. Natansohn and P. Rochon, *Chem. Rev.* **102**, 4139 (2002).
- [9] N.K. Viswanathan, D.Y. Kim, S. Bian, J. Williams, W. Liu, L. Li, L. Samuelson, J. Kumar and S.K. Tripathy, *J. Mater. Chem.* **9**, 1941 (1999).
- [10] T. Ubukata, M. Hara, K. Ichimura and T. Seki, *Adv. Mater.* **16**, 220 (2004).
- [11] H. Nakano, T. Takahashi, T. Kadota and Y. Shirota, *Adv. Mater.* **14**, 1157 (2002).
- [12] F. You, M.Y. Paik, M. Häckel, L. Kador, D. Kropp, H.W. Schmidt and C.K. Ober, *Adv. Funct. Mater.* **16**, 1577 (2006).
- [13] M.S. Ho, A. Natansohn and P. Rochon, *Macromolecules* **28**, 6124 (1995).
- [14] M.S. Ho, C. Barret, J. Paterson, M. Esteghamatian, A. Natansohn and P. Rochon, *Macromolecules* **29**, 4613 (1996).
- [15] D. Brown, A. Natansohn and P. Rochon, *Macromolecules* **28**, 6116 (1995).
- [16] X. Meng, A. Natansohn, C. Barrett and P. Rochon, *Macromolecules* **29**, 946 (1996).

- [17] Y. Wu, Q. Zhang, A. Kanazawa, T. Shiono, T. Ikeda and Y. Nagase, *Macromolecules* **32**, 3951 (1999).
- [18] V. Börger, O. Kuliskovska, J. Stumpe, M. Huber and H. Menzel, *Macromol. Chem. Phys.* **206**, 1488 (2005).
- [19] S. Hvilsted, F. Andruzzi, C. Kulinna, H.W. Siesler and P.S. Ramanujam, *Macromolecules* **28**, 2172 (1995).
- [20] Y. Wu, Y. Demachi, O. Tsutsumin, A. Kanazawa, T. Shiono and T. Ikeda, *Macromolecules* **31**, 1104 (1998).
- [21] F.L. Labarthe, S. Freiberg, C. Pellerin, M. P-zolet, A. Natansohn and P. Rochon, *Macromolecules* **33**, 6815 (2000).
- [22] C. Battett, B. Choudhury, A. Natansohn and P. Rochon, *Macromolecules* **31**, 4845 (1998).
- [23] M. Helgert, L. Wenke, S. Hvilsted and P.S. Ramanujam, *Appl. Phys. B* **72**, 429 (2001).
- [24] Y. He, X. Wang and Q. Zhou, *Polymer* **43**, 7325 (2002).
- [25] Y. He, J. Yin, P. Che and X. Wang, *Eur. Polym. J.* **42**, 292 (2006).
- [26] M.J. Kim, J. Lee, C. Chun, D.Y. Kim, S. Higuchi and T. Nakayama, *Macromol. Chem. Phys.* **208**, 1753 (2007).
- [27] P. Bortolus and S. Monti, *J. Phys. Chem.* **83**, 648 (1979).
- [28] T. Nägele, R. Hoche, W. Zinth and J. Wachtveitl, *Chem. Phys. Lett.* **272**, 489 (1997).
- [29] I.K. Lednev, T.Q. Ye, P. Matousek, M. Towrie, P. Foggi, F.V.R. Neuwahl, S. Umaphathy, R.E. Hester and J.N. Moore, *Chem. Phys. Lett.* **290**, 68 (1998).
- [30] H. Rau, in *Photochromism: Molecules and System*, edited by H. Durr and H. Bouas-Laurent (Elsevier, Amsterdam, 1990), Vol. 1, Chapt. 4, pp. 165–192, and references therein.
- [31] H. Rau and E. Lueddecke, *J. Am. Chem. Soc.* **104**, 1616 (1982).
- [32] E.W. Diau, *J. Phys. Chem. A* **108**, 950 (2004).
- [33] Y. Dou, Y. Hu, S. Yuan, W. Wu and H. Tang, *Mol. Phys.* **107**, 181 (2009).
- [34] Y. Dou, B.R. Torralva and R.E. Allen, *J. Mod. Opt.* **50**, 2615 (2003).
- [35] Y. Dou, B.R. Torralva and R.E. Allen, *Chem. Phys. Lett.* **392**, 352 (2004).
- [36] M. Graf and P. Vogl, *Phys. Rev. B* **51**, 4940 (1995).
- [37] T.B. Boykin, R.C. Bowen and G. Klimeck, *Phys. Rev. B* **63**, 245314 (2001).
- [38] D. Porezag, T. Frauenheim, T. Kohler, D. Seifert and R. Kaschner, *Phys. Rev. B* **51**, 12947 (1995).
- [39] M. Elstner, D. Porezag, G. Jungnickel, J. Elsner, M. Haugk, T. Frauenheim, S. Suhai and G. Seifert, *Phys. Rev. B* **58**, 7260 (1998).
- [40] R.E. Allen, T. Dumitrica and B.R. Torralva, in *Ultrafast Physical Processes in Semiconductors*, edited by K.T. Tsen (Academic Press, New York, 2001), Chapt. 7, pp. 315–386.
- [41] M. Born and J.R. Oppenheimer, *Ann. Phys. (Leipzig)* **84**, 457 (1927).
- [42] M. Born and K. Huang, *The Dynamical Theory of Crystal Lattices* (Oxford University Press, London, 1954).
- [43] E. Teller, *J. Phys. Chem.* **41**, 109 (1937).
- [44] W. Domcke, D.R. Yarkony and H. Köppel, *Conical Intersections: Electronic Structure, Dynamics and Spectroscopy* (World Scientific, Singapore, 2004).
- [45] M. Baer, *Beyond Born–Oppenheimer: Electronic Nonadiabatic Coupling Terms and Conical Intersections* (Wiley Interscience, Hoboken, 2006).
- [46] P. Cattaneo and M. Persico, *Phys. Chem. Chem. Phys.* **1**, 4739 (1999).
- [47] T. Ishikawa, T. Noro and T. Shoda, *J. Chem. Phys.* **115**, 7503 (2001).
- [48] M.L. Tiago, S. Ismail-Beigi and S.G. Louie, *J. Chem. Phys.* **122**, 094311 (2005).
- [49] C. Ciminelli, G. Granucci and M. Persico, *Chem. Eur. J.* **10**, 2327 (2004).
- [50] C. Chang, Y. Lu, T. Wang and E.W. Diau, *J. Am. Chem. Soc.* **126**, 10109 (2004).
- [51] B. Schmidt, C. Sobotta, B. Heinz, S. Laimgruber, M. Braun and P. Gilch, *Biochim. Biophys. Acta.-Bioenerg.* **1706**, 165 (2005).
- [52] S. Yuan, Y. Dou, W. Wu, Y. Hu and J. Zhao, *J. Phys. Chem. A* **112**, 13326 (2008).